

Simultaneous Compression and Absorption for Energy-Efficient Dissolution of Gases in Liquid

Evgenia Giakoumatou, Ann-Kathrin Goßmann, Björn Stelzner*, and Dimosthenis Trimis

DOI: 10.1002/cite.202100153

 This is an open access article under the terms of the Creative Commons Attribution License, which permits use, distribution and reproduction in any medium, provided the original work is properly cited.

Dedicated to Prof. Dr. Thomas Hirth on the occasion of his 60th birthday

In this study, a novel approach for energy-efficient dissolution of gases in liquid is presented, which significantly reduces the compression work. The core of the one-step process is the simultaneous operation of compression and absorption. The liquid was injected into a cylinder filled with the gas, while a piston compressed the mixture during the injection time. The solubility increases with increasing system pressure, so that the compression work of the gas phase is permanently reduced on the one hand by the permanent reduction of the gas volume and on the other hand by the nearly isothermal compression process. The approach is demonstrated in this study using liquid H₂O and gaseous CO₂ compressed up to 10 bar. The theoretical energy savings of the novel process compared to the conventional two-stage process is 41.2 % for the selected fluids. A maximum energy saving of 40.8 % was demonstrated in the experiments. The results also show that the energy saving depends on the curve of the piston speed and the injection time.

Keywords: Absorption, Compression, Dissolution, Energy efficiency, Gas in liquid

Received: July 31, 2021; *revised:* December 15, 2021; *accepted:* January 18, 2022

1 Introduction

The CO₂ dissolution in water or aqueous mixtures at different temperature and pressure conditions is of great importance for various environmental, geochemical, industrial and thermodynamic problems [1]. Fundamental experimental data was obtained already decades ago [2], and research on the dissolution of CO₂ in pure water or in aqueous solution systems is still ongoing in recent years [3–5]. These data are needed in various research areas, e.g., to quantify the feedback between ocean warming and CO₂ solubility as an equivalent carbon emission [6] or for carbon capture and storage concepts [7]. Many works are concerned with subsurface disposal of CO₂, where much of the CO₂ is dissolved in reservoir water. An overview of relevant work in this area is given by Holloway [8].

Kaliyan et al. [9] give an overview of applications of CO₂ in the food industry. In those technical applications, the solution process of gas in liquid is realized in a conventional way, in which the gas phase is compressed at an advanced stage. Although in many cases the heat of compression is dissipated unused, there are examples where heat recovery can be used to increase the efficiency of the compression process [10]. The processes for dissolving gases in liquids are based on compression and subsequent dissolution of the gas. The compression of the pure gas in a first step reflects the fundamental inefficiency in terms of the heat of compression generated in the isentropic process. Here, all the

energy spent on gas compression is partially converted into heat.

In this study, a novel approach to simultaneous compression and absorption for energy-efficient dissolution of gases in liquids is presented.

2 Concept of the Novel Approach

The currently existing processes for dissolving gases in solvents are based on compression and subsequent dissolution of the gas. In this case, the energy demand of the process is dominated by the compression phase, which can be approximated as an isentropic process. The idea of the proposed concept is to perform the compression of a gas in the presence of the solvent, which has a positive effect on the energy demand of the compression process in two ways:

- 1) The effect of increasing solubility of the gas in liquid with increasing pressure leads to a progressive dissolution of the gas during the compression process and thus

Evgenia Giakoumatou, Ann-Kathrin Goßmann, Björn Stelzner, Dimosthenis Trimis
bjoern.stelzner@kit.edu
Karlsruhe Institute of Technology, Engler-Bunte-Institute, Combustion Technology, Engler-Bunte-Ring 7, 76131 Karlsruhe, Germany.

to a reduction in the amount of gas that must be compressed at any given time, assuming saturation.

- Due to its high heat capacity, the solvent present can absorb large amounts of heat without significant temperature rises, which leads to an approximately isothermal process.

In the present study, this concept is demonstrated with CO₂ as gas and H₂O as solvent. To implement the concept for technical applications, an injector is integrated into a reciprocating compressor to create a fine spray in the compression chamber. The spray leads to a large increase of the liquid surface and promotes the dissolution process of the gas.

Fig. 1 shows the proposed operation of the reciprocating compressor modified to perform compression with simultaneous dissolution. An example duty cycle begins with the piston at top dead center (TDC). In the first step (a), the compression chamber is filled with CO₂ from a low-pressure vessel (ambient conditions). Then the solvent is injected (b) and the two-phase mixture is compressed (c) until saturation is reached and only the liquid solution remains. At the end of the cycle, the liquid solution is forced out by moving the piston to TDC (d).

3 Theoretical Background

As described above, the concept of the presented approach compared to conventional dissolution processes is the suppression of a temperature increase of the gas phase due to heat of compression and the continuous decrease of the gas volume due to dissolution during compression. The ideal process is defined below, with the following assumptions:

- saturation at any time of the process, i.e., the smallest possible amount of CO₂ is in the gas phase,
- isothermal conditions.

The various compression processes are shown schematically in a p - v diagram in Fig. 2.

Assuming that CO₂ is an ideal gas, which is a reasonable assumption for the relevant pressure range, the pressure in the compression chamber as a function of the stroke dis-

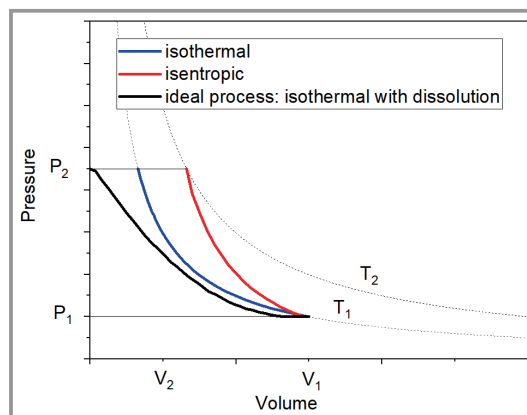


Figure 2. Schematic representation of the compression processes in the p - v diagram.

tance from the bottom dead center (BDC) can be expressed by Eq. (1), where $V_{\text{H}_2\text{O}}(h)$ is the amount of solvent in the compression chamber at the stroke position h . It is assumed that the solvent is introduced either at the beginning or during the compression process.

$$p(h) = \frac{n_{\text{CO}_2}^0 R T_0}{A(h_{\text{stroke}} - h) + (k_{\text{H}} R T_0 - 1)V_{\text{H}_2\text{O}}(h)} \quad (1)$$

The work for compression can be calculated by Eq. (2), where the residual amount of CO₂ in the gas phase is given by Eq. (3).

$$W = \int_{p_0}^{p_p} V dp = \int_{p_0}^{p_p} \frac{n(p)RT_0}{p} dp \quad (2)$$

$$n(p) = n_{\text{CO}_2}^0 - k_{\text{H}} V_{\text{H}_2\text{O}} p \quad (3)$$

As already mentioned, the common method for the dissolution of CO₂ in a solvent is the compression of the gaseous CO₂ followed by dissolution. Therefore, in terms of

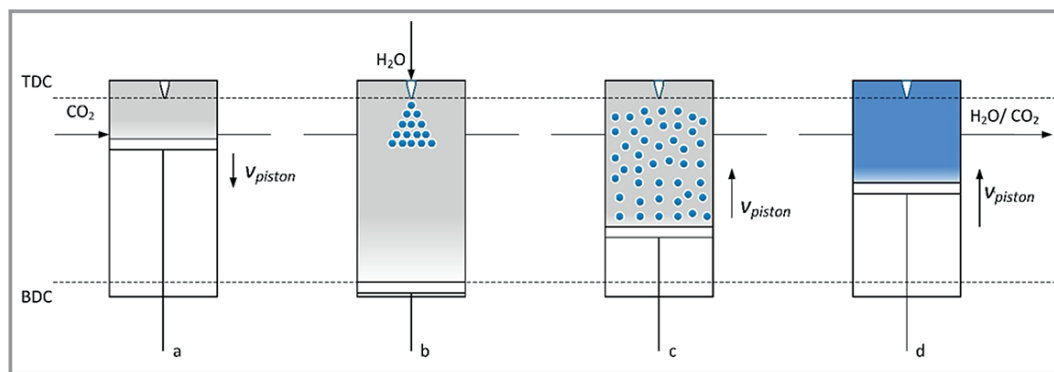


Figure 1. Schematic duty cycle of the process.

energy saving, the process to be compared is isentropic compression. The work for the isentropic compression is calculated using Eqs. (4) and (5).

$$W_{\text{is,CO}_2} = \frac{\gamma p_0 V_0}{\gamma - 1} \left(\left(\frac{p_p}{p_0} \right)^{\frac{\gamma-1}{\gamma}} - 1 \right) \quad (4)$$

$$W_{\text{is,H}_2\text{O}} = V_{\text{H}_2\text{O}} \Delta p \quad (5)$$

The solubility of a substance depends essentially on the chemical properties of the solute and the solvent (pH, polarity of the molecules, chemical bonds) and on physical properties such as temperature and pressure. In this case, we are concerned with the analysis of the dissolution of gases in a liquid, in particular CO₂ in water. This subject was studied in detail in the early 19th century by William Henry [11]. According to Henry's law (Eq. (1)), the amount of a given gas dissolved in a liquid at constant pressure is directly proportional to the partial pressure of the gas at equilibrium with the liquid.

$$p = k_H(T)x \quad (6)$$

where p is the partial pressure of the solute in the solution, x is the concentration of the solute in the solution, $k_H(T)$ is Henry's law constant as a function of temperature, usually expressed in (atm mol⁻¹). The effect of the temperature is expressed by the Van't-Hoff equation, shown in Eq. (2),

$$k_H(T) = k_H^0 \exp \left(-C \left(\frac{1}{T} - \frac{1}{T^0} \right) \right) \quad (7)$$

where C is a constant measured in (K) and T^0 is the standard temperature. A large collection of values for the Henry coefficient in water can be found in [12].

Using Eq. (8) and the two reference cases defined previously, a measure can be defined to evaluate the experimental results. This measure is called the process efficiency η . An efficiency of $\eta = 1$ corresponds to the ideal case, while an efficiency of $\eta = 0$ represents the isentropic gas compression.

$$\eta = 1 - \frac{\Delta W}{\Delta W_{\text{is}}} \quad (8)$$

with

$$\Delta W = W_{\text{exp}} - W_{\text{ideal}} \quad (9)$$

and

$$\Delta W_{\text{is}} = W_{\text{is}} - W_{\text{ideal}} \quad (10)$$

4 Experimental Setup

The compression/dissolution was performed as a batch process. A cylinder was filled with CO₂ at atmospheric conditions. Water was injected into the cylinder while compression started with a piston. In the final step, the liquid water/CO₂ solution is ejected at a final pressure of 10 bar_g.

In this work, an acrylic cylinder with a total length of 725 mm and an inner diameter of 125 mm was used. A high-pressure piston pump was used to pressurize the water up to 60 bar. A pressurized atomizer (full cone) with a diameter of 1.70 mm and a spray angle of 60° was applied. The differential pressure changed during the experiment between 59 bar (start of compression) and 49 bar (end of compression) and consequently, the flow rate of the water, which was determined experimentally, varied between 0.12 L s⁻¹ and 0.13 L s⁻¹.

An unloader valve and a pressure sensor were installed upstream of the nozzle to control the liquid pressure upstream of the atomizer. In addition, a solenoid valve was mounted in the line to control the liquid injection time. The maximum stroke used in this study was 600 mm, resulting in a total volume of 7.36 L. The internal pressure was measured with a pressure sensor (0 to 16 bar_g) and the internal temperature was monitored with a K-type thermocouple. Downstream, a pressure relief valve was placed to measure the pressure curves up to 10 bar. The solution was then collected in a membrane expansion vessel where it can be stored under high pressure.

The compressor is equipped with several sensors for measuring the process parameters, temperature, and pressure during or at the end of the compression process. In addition, there is a magnetostrictive sensor for piston position on the hydraulic side of the compressor. With this sensor, the piston speed can be determined over the stroke and the measured process parameters can be assigned to the respective piston position. The characteristics of the experimental setup are shown in Tab. 1.

Table 1. Characteristics of the experimental setup.

Compressor parameters	Value
<i>Hydraulic cylinder</i>	
Piston diameter [mm]	140
Stern diameter [mm]	70
Stroke [mm]	600
<i>CO₂/solvent compression chamber</i>	
Piston diameter [mm]	125
Stern diameter [mm]	70
Stroke [mm]	600
<i>Hydraulic unit</i>	
Motor power [kW]	7.5
Motor control	Inverter

5 Results and Discussion

5.1 Characterization of the Spray

A two-color phase Doppler anemometry (PDA) system was used to characterize the spray. The axial and radial velocity components and the diameter of each droplet were determined. The PDA system was operated in first-order refractive mode at a scattering angle of 30° . Two diode lasers with green and yellow light, each with a power of about 150 mW, were sent through the transmitting optics with a focal length of 500 mm. The optical arrangement resulted in a measurement volume with a diameter of about $240\ \mu\text{m}$ and a length of about $3500\ \mu\text{m}$. The receiving probe was equipped with a lens with a focal length of 500 mm and an effective spatial filter width of $400\ \mu\text{m}$. With the setup used, a maximum droplet diameter of $300\ \mu\text{m}$ could be determined. The PDA system was mounted on a traverse system in order to scan the spatial spray characteristics. At each measured position, 40 000 samples were taken at a data rate of about 10 kHz.

Results of the spraying process are presented in Fig. 3, where the radial distribution of the SMD is shown for different heights and two different inlet pressures. The two inlet pressures represent the start of the compression (60 bar) and the end of the compression (50 bar).

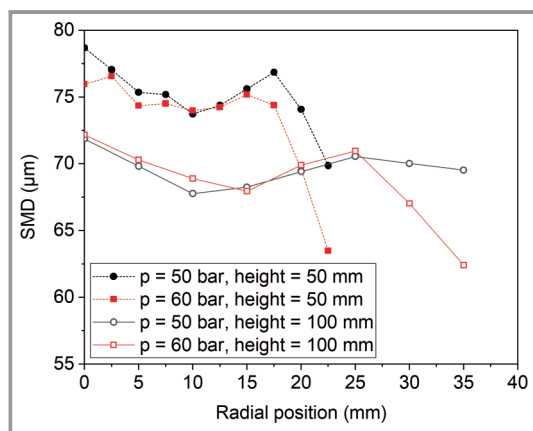


Figure 3. Radial distribution of the SMD at two heights and two inlet pressures.

The results show that even when the pressure is changed, there is no significant effect on the SMD. The spray exhibits the highest SMD of $78\ \mu\text{m}$ near the nozzle at a height of 50 mm and drops to $64\ \mu\text{m}$ in the radial direction. Further upstream, at a height of 100 mm, the spray exhibits an almost constant SMD of about $70\ \mu\text{m}$. This indicates a large surface increase of the water in order to promote the CO_2 dissolution.

5.2 Compression/Dissolution

The inlet pressure of the nozzle was set at 60 bar, resulting in a flow rate of H_2O of $9.9\ \text{L min}^{-1}$. The injection time was 7.14 s in all cases, so the total amount of H_2O injected was 1.8 L. In this quantity, the total CO_2 volume of 7.14 L (standard conditions at the beginning of compression) is theoretically completely dissolved at a system pressure of 6 bar.

In the present study, three different cases were investigated, which were distinguished by a delay time in the injection of H_2O after the start of compression. In case 1 there was no time delay, in case 2 a time delay of 2.04 s and in case 3 of 3.16 s. The pressure curves as function of the piston position are shown in Fig. 4 in comparison with isentropic compression and the ideal case.

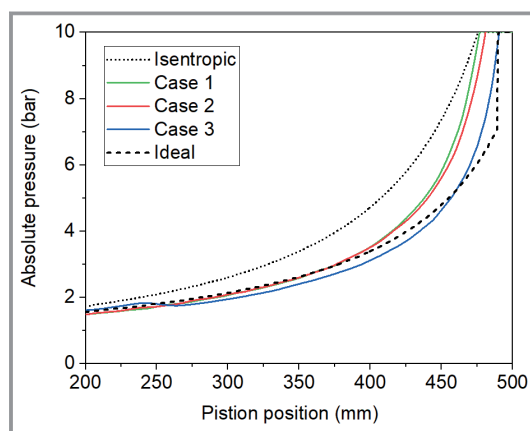


Figure 4. Pressure curves depending on the stroke.

The results show that all cases follow the ideal case with low pressure rise at the beginning of compression. Here, the influence of the heat of compression is marginal compared to the rapid pressure increase at the end of each test. Therefore, the time delay between start of compression and start of injection can be used to shift the H_2O injection towards the end of the compression.

The comparison of the work consumption is shown in Fig. 5 for the calculated isentropic and ideal compression process as well as for the three experiments. As expected, the work consumption is highest in the isentropic case with 2943 J. The ideal case reduces the work consumption to 1736 J. Case 3 with the largest delay time of the H_2O injection showed the best reduction in work consumption at 1749 J. This supports the finding that the application of the present approach requires a focus on the final stage of compression, where a large pressure rise occurs.

6 Conclusion

In the present study, a novel approach for energy-efficient dissolution of gases in the liquid dissolution process was

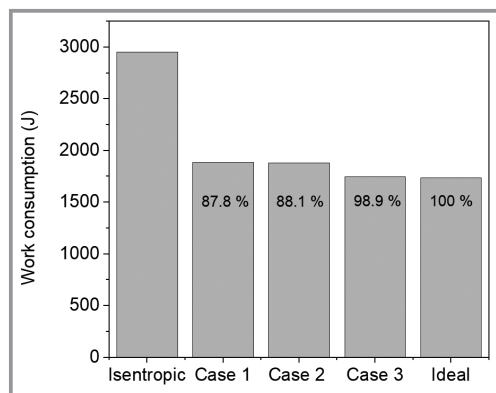


Figure 5. Comparison of the work consumption.

presented using the liquids CO₂ and H₂O as examples. It was shown that simultaneous injection of a fluid with a much higher heat capacity than the gas and compression avoided a density change of the gas due to the heat of compression. In addition, the continuous dissolution of the gas in the solvent reduced the gas volume and thus the compression work of the gas phase. The largest reduction of the work consumption can be achieved in the final stage of the compression. In the experiments, a high process efficiency between about 88 % and 99 % was realized.

This project was supported by funding from the European Union's Horizon 2020 research and innovation program under grant agreement No. 679050 - CELBICON. In addition, the authors would like to acknowledge financial support from the German Research Foundation (DFG) for measurement equipment under the HBFG program INST121384/178-1 FUGG. Open access funding enabled and organized by Projekt DEAL.

Symbols used

A	[mm ²]	surface
c	[K]	constant
h	[mm]	position
k_H	[mol kg ⁻¹ bar ⁻¹]	Henry constant
n	[mol]	number of moles
p	[bar]	pressure
R	[m ³ Pa mol ⁻¹ K ⁻¹]	ideal gas constant
T	[K]	temperature
V	[mm ³]	volume
W	[J]	work

Greek letters

γ	[-]	isentropic expansion factor
η	[-]	efficiency

Sub- and Superscripts

a	absolute
g	gauge

Abbreviations

BDC	bottom dead center
PDA	phase Doppler anemometry
SMD	Sauter mean diameter
TDC	top dead center

References

- [1] A. Hemmati-Sarapardeh, M. N. Amar, M. R. Soltanian, Z. Dai, X. Zhang, *Energy Fuels* **2020**, *34* (4), 4761–4776. DOI: <https://doi.org/10.1021/acs.energyfuels.0c00114>
- [2] S. Takenouchi, G. C. Kennedy, *Am. J. Sci.* **1964**, *262* (9), 1055–1074. DOI: <https://doi.org/10.2475/ajs.262.9.1055>
- [3] H. Teng, A. Yamasaki, *Chem. Eng. Commun.* **2002**, *189* (11), 1485–1497. DOI: <https://doi.org/10.1080/00986440214993>
- [4] G. Ferrentino, D. Barletta, F. Donsi, G. Ferrari, M. Poletto, *Ind. Eng. Chem. Res.* **2010**, *49* (6), 2992–3000. DOI: <https://doi.org/10.1021/ie9009974>
- [5] Y. Liu, M. Hou, G. Yang, B. Han, *J. Supercrit. Fluids* **2011**, *56* (2), 125–129. DOI: <https://doi.org/10.1016/j.supflu.2010.12.003>
- [6] P. Goodwin, T. M. Lenton, *Geophys. Res. Lett.* **2009**, *36* (15), L15609. DOI: <https://doi.org/10.1029/2009GL039247>
- [7] M. L. Szulczewski, C. W. MacMinn, H. J. Herzog, R. Juanes, *Proc. Natl. Acad. Sci. U.S.A.* **2012**, *109* (14), 5185–5189. DOI: <https://doi.org/10.1073/pnas.1115347109>
- [8] S. Holloway, *Energy Convers. Manage.* **1997**, *38* (1), 193–198. DOI: [https://doi.org/10.1016/s0196-8904\(96\)00268-3](https://doi.org/10.1016/s0196-8904(96)00268-3)
- [9] N. Kaliyan, P. Gayathri, K. Alagusundaram, R. V. Morey, W. F. Wilcke, *ASAE Annual Meeting*, Minneapolis, MN **2007**. DOI: <https://doi.org/10.13031/2013.23553>
- [10] X. She, X. Peng, B. Nie, G. Leng, X. Zhang, L. Weng, L. Tong, L. Zheng, L. Wang, Y. Ding, *Appl. Energy* **2017**, *206*, 1632–1642. DOI: <https://doi.org/10.1016/j.apenergy.2017.09.102>
- [11] W. Henry, Experiments on the quantity of gases absorbed by water, at different temperatures, and under different pressure, *Philos. Trans. R. Soc. London* **1803**, *83*, 29–42. DOI: <https://doi.org/10.1098/rstl.1803.0004>
- [12] R. Sander, *Atmos. Chem. Phys* **2015**, *15*, 4981–4981. DOI: <https://doi.org/10.5194/acp-15-4399-2015>

DOI: 10.1002/cite.202100153

Simultaneous Compression and Absorption for Energy-Efficient Dissolution of Gases in Liquid

Evgenia Giakoumatou, Ann-Kathrin Gofsmann, Björn Stelzner, Dimosthenis Trimis*

Research Article: A novel approach to dissolve gases in liquids at elevated pressure with high energy efficiency is presented. Simultaneous absorption and compression continuously reduces the required compression work of the gas phase and the presence of liquid lowers the heat of compression to a near isothermal process. An energy reduction of 41 % was achieved.

